

# Inverse- $k$ Primordial Oscillations from a Symbolic Regression Search

Ze-Yu Peng,<sup>1,2,\*</sup> Qing-Yu Lan,<sup>1,†</sup> and Yun-Song Piao<sup>1,2,3,4,‡</sup>

<sup>1</sup>*School of Physical Sciences, University of Chinese Academy of Sciences, Beijing 100049, China*

<sup>2</sup>*International Centre for Theoretical Physics Asia-Pacific,  
University of Chinese Academy of Sciences, 100190 Beijing, China*

<sup>3</sup>*School of Fundamental Physics and Mathematical Sciences,*

*Hangzhou Institute for Advanced Study, UCAS, Hangzhou 310024, China*

<sup>4</sup>*Institute of Theoretical Physics, Chinese Academy of Sciences, P.O. Box 2735, Beijing 100190, China*

Oscillatory features in the primordial power spectrum, potential signatures of new physics in the early universe, are usually searched for using fixed templates. In this work, we perform a template-free search for primordial features using symbolic regression. We find that both Planck and the combined Planck+ACT+SPT-3G datasets independently select an inverse- $k$  oscillation,  $\cos(B/k)$  with  $B \simeq 4 \text{ Mpc}^{-1}$ , as the leading low-complexity feature. Comparing this inverse- $k$  template with standard linear and logarithmic oscillating templates, we find that it fits the data best, showing a weak preference for a non-zero amplitude. Our results show that symbolic regression as a powerful machine learning technique can provide an interpretable, model-independent approach to cosmological discovery.

*Introduction.*— Inflation [1–4], the standard paradigm of the very early universe, predicts a nearly scale-invariant primordial power spectrum (PPS) of scalar perturbations, which is in good agreement with the Planck cosmic microwave background (CMB) observations [5]. Nevertheless, departures from the slow-roll dynamics can imprint oscillatory features on the PPS [6–11], while remaining consistent with current observations. The search for such features offers a unique window into the new physics in the primordial universe [12, 13].

Previous searches for primordial oscillatory features have mostly used linear and logarithmic oscillation templates, and have found no evidence for a departure from the power-law spectrum [14–23]. The tightest constraint to date comes from the combination of Planck with the latest ACT [24, 25] and SPT-3G [26] data [27, 28]. See also [29–33] for constraints on other realistic models of primordial features.

Symbolic regression (SR) [34, 35] has emerged as a powerful tool for scientific discovery. By searching for explicit analytical expressions that optimize a given objective, SR enables the discovery of interpretable models directly from data without relying on predefined functional forms or black-box approximators. SR has been shown to rediscover known physical laws directly from experimental data [36]. It has recently been applied to a variety of problems in cosmology, e.g. [37, 38] for the reconstruction of the expansion history and [39] for an exhaustive SR approach.

In this work, we perform a template-free search for primordial features using SR. We consider Planck and its combination with the latest ACT and SPT-3G data, and find that both datasets independently select an inverse- $k$  oscillation,  $\cos(B/k)$  with  $B \simeq 4 \text{ Mpc}^{-1}$ , as the leading low-complexity feature. We further compare this inverse- $k$  template with the standard linear and logarithmic templates, and find that it fits the data better and shows a

Complexity	$\Delta\chi^2_{\text{Planck}}$	$f(k)$
8	−9.69	$-0.0299 \cos(4.101/k)$
10	−11.44	$-0.0339 \cos(4.150/k - 0.859)$
11	−13.10	$k \sin(-0.868/k^2)$
16	−21.35	$0.0924 \sin[(2.990 + 0.5248/k)/k]$

TABLE I. Pareto-front expressions from the Planck symbolic-regression run. The improvement  $\Delta\chi^2$  is measured relative to the no-feature power-law spectrum.

weak preference for a nonzero amplitude, while the standard templates remain consistent with zero.

*Methods and datasets.*— We write the primordial power spectrum (PPS) as

$$P_{\mathcal{R}}(k) = P_{\mathcal{R},0}(k) [1 + f(k)], \quad P_{\mathcal{R},0}(k) = A_s \left( \frac{k}{k_*} \right)^{n_s-1}, \quad (1)$$

with  $k_* = 0.05 \text{ Mpc}^{-1}$ . Here  $f(k)$  is the primordial feature we search for, and  $f(k) = 0$  recovers the standard power-law spectrum  $P_{\mathcal{R},0}$ .

We search for analytic expressions for  $f(k)$  using symbolic regression as implemented in PySR [35], with the CMB  $\chi^2$  as the loss function. The CMB spectra are computed using CLASS [40], and all the cosmological and nuisance parameters are fixed to their best-fit values for the standard power-law spectrum. See Supplemental Material [41] for details of the SR search.

We consider two CMB datasets, Planck and SPA (Planck+SPT+ACT). The Planck dataset includes the full high- $\ell$  Plik-lite TTTEEE and low- $\ell$  Commander TT likelihoods [5]. The SPA dataset combines the SPT-3G D1 [26] and ACT DR6 [24, 25] data with Planck. Following [24, 26], the Planck high- $\ell$  data in SPA are cropped to  $\ell_{\text{max}} = 1000$  for TT and 600 for TE and EE; we further restrict SPT and ACT to  $\ell \leq 2500$ , matching the scales of Planck and avoiding the modeling uncertainties at smaller scales [42, 43].

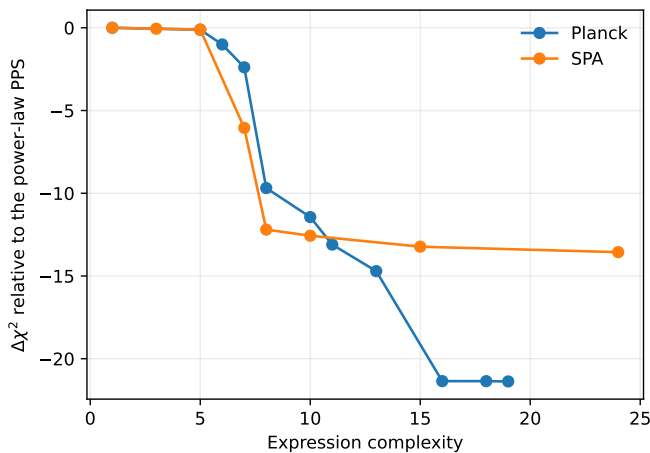


FIG. 1. Improvement of the CMB likelihood along the SR Pareto front relative to the standard power-law spectrum.

*SR results.*—

Complexity	$\Delta\chi_{\text{SPA}}^2$	$f(k)$
7	-6.05	$-0.0106 \sin(-390.0k)$
8	-12.20	$-0.0209 \sin(4.231/k)$
10	-12.57	$0.0209 \sin(4.178/k - 2.594)$
15	-13.23	$0.0218 \sin(4.173/k + 4.173/e^k)$

TABLE II. Pareto-front expressions from the SPA symbolic-regression run. The improvement  $\Delta\chi^2$  is measured relative to the no-feature power-law spectrum.

In Fig. 1, we show the Pareto fronts obtained from the SR search for the Planck and SPA datasets, with some representative expressions listed in Tables I and II; the complete results are given in Supplemental Material [41]. For both datasets, the likelihood improvement slows down around complexity 8 (C8), where the two runs converge to the same form, an inverse- $k$  oscillation with similar frequency,

$$f_{\text{Planck}}^{(8)}(k) \simeq -0.0299 \cos\left(\frac{4.101}{k}\right), \quad (2)$$

$$f_{\text{SPA}}^{(8)}(k) \simeq -0.0209 \sin\left(\frac{4.231}{k}\right), \quad (3)$$

with  $k$  measured in  $\text{Mpc}^{-1}$ .

Beyond C8, the two datasets behave differently. For SPA, the front saturates: the higher-complexity C10, C15 and C24 expressions are essentially the same inverse- $k$  oscillation, differing at most by a small  $e^{-k}$  term in the phase. For Planck, the likelihood keeps improving, but the additional gain comes from inverse-power terms such as  $1/k^2$ , which oscillate increasingly rapidly toward small  $k$  and fall below the sampling resolution of our CLASS runs; we therefore treat these high-complexity Planck expressions as numerically unreliable, see details in Supplemental Material [41].

In Fig. 2, we show the CMB residuals of the C8 expressions, projected from the PPS to the TT, TE and EE spectra relative to the SPA power-law baseline. The Planck and SPA expressions yield a similar oscillatory pattern over the range  $800 \lesssim \ell \lesssim 2000$ , which tracks the oscillations in the measured residuals from SPT and ACT, most clearly in the TE and EE polarization spectra.

*Comparison with standard templates.*— The SR search suggests an inverse- $k$  oscillation in the PPS. We compare it with the commonly used linear and logarithmic oscillation templates.

Parameter	Prior
$A_X$	$[0, 0.5]$
$\omega_X$	$[1, 100]$
$\phi_X$	$[0, 2\pi]$

TABLE III. Priors for the three templates

The three templates of primordial features are defined as

$$f_X(k) = A_X \cos[\omega_X g_X(k) + \phi_X], \quad (4)$$

with

$$g_{\text{lin}}(k) = \frac{k}{k_*}, \quad g_{\text{log}}(k) = \log \frac{k}{k_*}, \quad g_{\text{inv}}(k) = \frac{k_*}{k}. \quad (5)$$

We use the same flat priors for all three templates, listed in Table III[44]. For each template, we run a separate Markov chain Monte Carlo (MCMC) analysis over  $(A_X, \omega_X, \phi_X)$  on the SPA dataset using Cobaya [45], with the background and nuisance parameters fixed as in the SR search. It has been shown that the variation of the background and nuisance parameters has a negligible effect on the feature constraints [27].

Figure 3 shows the marginalized posteriors of the amplitude  $A_X$ . We find a  $1\sigma$  lower bound for the amplitude of the inverse- $k$  template,  $A_X = 0.0163_{-0.0071}^{+0.0099}$ , showing a weak preference for a nonzero amplitude, while the linear and logarithmic templates are consistent with zero and give only upper limits.

The best-fit  $\chi^2$  values are summarized in Table IV. All three templates improve over the no-feature baseline, but the inverse- $k$  template gives the largest improvement,  $\Delta\chi^2 \simeq -12.6$ , against  $-7.69$  for the linear and  $-5.8$  for the logarithmic template. This improvement is dominated by the small-scale SPT-3G and ACT data. The corresponding CMB residuals are shown in Fig. 4.

*Discussion.*— The search for primordial features offers a unique window into the new physics of the primordial universe. In this work, we have performed a template-free search for primordial features using symbolic regression. For both Planck and its combination with the latest ACT and SPT-3G data, the search independently selects an inverse- $k$  oscillation as the leading low-complexity feature. We further compare this inverse- $k$  template with

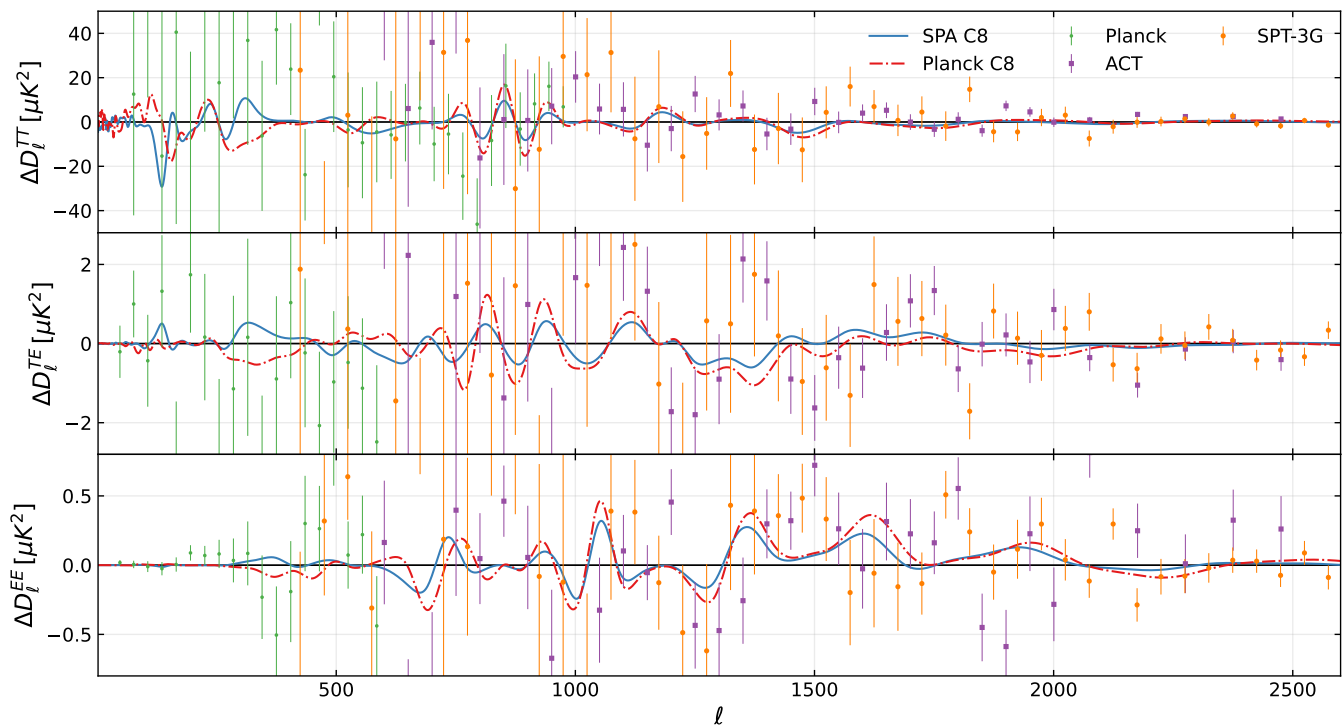


FIG. 2. CMB residuals for SR expressions with complexity 8, relative to the SPA power-law baseline. We also show the Planck (cropped), ACT and SPT-3G data bins.

Template	$A_X$	$\omega_X$	$\phi_X$	$\Delta\chi^2$	Planck	SPT-3G	ACT
baseline	0	—	—	0.00	243.76	109.90	110.29
linear	0.0113	18.69	6.00	-7.69	239.26	108.64	108.35
log	0.0309	83.14	1.64	-5.85	241.51	110.40	106.18
inverse	0.0203	83.32	2.24	-12.66	240.78	103.94	106.55

TABLE IV. Best-fit template parameters and component  $\chi^2$  values for the SPA dataset.

the standard linear and logarithmic oscillation templates using MCMC. We find a weak preference for a nonzero amplitude for the inverse- $k$  oscillation, while the standard templates remain consistent with zero.

According to the primordial standard-clocks formalism [12, 13], a  $k^{1/p}$  oscillation in the PPS can be generated by a massive field oscillating in a background with scale factor  $a(t) \sim t^p$ . Therefore, our inverse- $k$  oscillation may be interpreted as an early fast expansion phase with a slowly increasing Hubble parameter ( $p = -1$ ,  $t < 0$  and  $w < -1$ ), as may occur in NEC-violating or phantom-like early-universe scenarios [46–51]. It should be noted that we regard this connection as heuristic, since our results only identify the oscillation phase rather than the full standard-clocks signal. Specific model implementation and observational tests are left for future work.

Our results demonstrate that symbolic regression provides a useful and complementary approach to the search for primordial features, able to identify forms beyond the standard templates. It is expected that future CMB

experiments, such as the Simons Observatory [52] and CMB-S4 [53], which provide improved measurements on small scales, will further refine our understanding of primordial features.

This work is supported by NSFC, No.12475064, 12075246, National Key Research and Development Program of China, No. 2021YFC2203004, and the Fundamental Research Funds for the Central Universities. We acknowledge the use of high performance computing services provided by the International Centre for Theoretical Physics Asia-Pacific cluster.

\* pengzeyu23@mails.ucas.ac.cn  
† lanqingyu19@mails.ucas.ac.cn  
‡ yspiao@ucas.ac.cn

[1] A. H. Guth, *Phys. Rev. D* **23**, 347 (1981).  
[2] A. D. Linde, *Phys. Lett. B* **108**, 389 (1982).  
[3] A. Albrecht and P. J. Steinhardt, *Phys. Rev. Lett.* **48**,

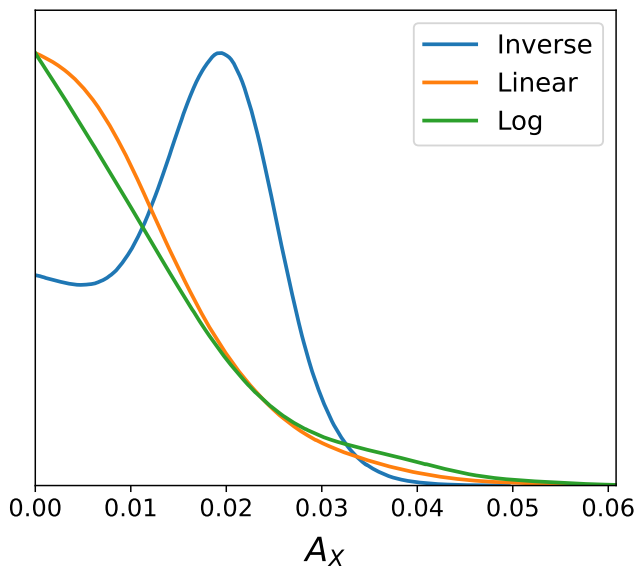


FIG. 3. Marginalized posteriors of the oscillation amplitude  $A_X$  for the linear, logarithmic and inverse- $k$  templates on the SPA dataset.

- 1220 (1982).
- [4] A. A. Starobinsky, *Phys. Lett. B* **91**, 99 (1980).
- [5] N. Aghanim *et al.* (Planck), *Astron. Astrophys.* **641**, A6 (2020), [Erratum: *Astron. Astrophys.* 652, C4 (2021)], arXiv:1807.06209 [astro-ph.CO].
- [6] A. A. Starobinsky, *JETP Lett.* **55**, 489 (1992).
- [7] J. A. Adams, B. Cresswell, and R. Easther, *Phys. Rev. D* **64**, 123514 (2001), arXiv:astro-ph/0102236.
- [8] X. Wang, B. Feng, M. Li, X.-L. Chen, and X. Zhang, *Int. J. Mod. Phys. D* **14**, 1347 (2005), arXiv:astro-ph/0209242.
- [9] J.-O. Gong, *JCAP* **07**, 015 (2005), arXiv:astro-ph/0504383.
- [10] A. Slosar *et al.*, *Bull. Am. Astron. Soc.* **51**, 98 (2019), arXiv:1903.09883 [astro-ph.CO].
- [11] A. Achúcarro *et al.*, (2022), arXiv:2203.08128 [astro-ph.CO].
- [12] X. Chen and C. Ringeval, *JCAP* **08**, 014 (2012), arXiv:1205.6085 [astro-ph.CO].
- [13] X. Chen, A. Loeb, and Z.-Z. Xianyu, *Phys. Rev. Lett.* **122**, 121301 (2019), arXiv:1809.02603 [astro-ph.CO].
- [14] R. Easther, W. H. Kinney, and H. Peiris, *JCAP* **05**, 009 (2005), arXiv:astro-ph/0412613.
- [15] P. D. Meerburg, D. N. Spergel, and B. D. Wandelt, *Phys. Rev. D* **89**, 063536 (2014), arXiv:1308.3704 [astro-ph.CO].
- [16] P. D. Meerburg and D. N. Spergel, *Phys. Rev. D* **89**, 063537 (2014), arXiv:1308.3705 [astro-ph.CO].
- [17] H. Peiris, R. Easther, and R. Flauger, *JCAP* **09**, 018 (2013), arXiv:1303.2616 [astro-ph.CO].
- [18] R. Easther and R. Flauger, *JCAP* **02**, 037 (2014), arXiv:1308.3736 [astro-ph.CO].
- [19] M. Aich, D. K. Hazra, L. Sriramkumar, and T. Souradeep, *Phys. Rev. D* **87**, 083526 (2013), arXiv:1106.2798 [astro-ph.CO].
- [20] Y. Akrami *et al.* (Planck), *Astron. Astrophys.* **641**, A10 (2020), arXiv:1807.06211 [astro-ph.CO].
- [21] F. Beutler, M. Biagetti, D. Green, A. Slosar, and B. Wallich, *Phys. Rev. Res.* **1**, 033209 (2019), arXiv:1906.08758 [astro-ph.CO].
- [22] M. Ballardini, F. Finelli, F. Marulli, L. Moscardini, and A. Veropalumbo, *Phys. Rev. D* **107**, 043532 (2023), arXiv:2202.08819 [astro-ph.CO].
- [23] T. Mergulhão, F. Beutler, and J. A. Peacock, *JCAP* **08**, 012 (2023), arXiv:2303.13946 [astro-ph.CO].
- [24] T. Louis *et al.* (Atacama Cosmology Telescope), *JCAP* **11**, 062 (2025), arXiv:2503.14452 [astro-ph.CO].
- [25] E. Calabrese *et al.* (Atacama Cosmology Telescope), *JCAP* **11**, 063 (2025), arXiv:2503.14454 [astro-ph.CO].
- [26] E. Camphuis *et al.* (SPT-3G), *Phys. Rev. D* **113**, 083504 (2026), arXiv:2506.20707 [astro-ph.CO].
- [27] Z.-Y. Peng and Y.-S. Piao, *Phys. Rev. D* **113**, 023544 (2026), arXiv:2507.17276 [astro-ph.CO].
- [28] S. K. Nerval, R. Hlozek, H. T. Jense, and J. R. Bond, (2026), arXiv:2606.28310 [astro-ph.CO].
- [29] M. Braglia, X. Chen, and D. K. Hazra, *JCAP* **06**, 005 (2021), arXiv:2103.03025 [astro-ph.CO].
- [30] M. Braglia, X. Chen, and D. K. Hazra, *Eur. Phys. J. C* **82**, 498 (2022), arXiv:2106.07546 [astro-ph.CO].
- [31] M. Braglia, X. Chen, and D. K. Hazra, *Phys. Rev. D* **105**, 103523 (2022), arXiv:2108.10110 [astro-ph.CO].
- [32] M. Braglia, X. Chen, D. K. Hazra, and L. Pinol, *JCAP* **03**, 014 (2023), arXiv:2210.07028 [astro-ph.CO].
- [33] C. Petretti, M. Braglia, X. Chen, D. Kumar Hazra, and S. Paban, *JCAP* **06**, 035 (2025), arXiv:2411.03459 [astro-ph.CO].
- [34] M. Schmidt and H. Lipson, *Science* **324**, 81 (2009).
- [35] M. Cranmer, “Interpretable machine learning for science with pysr and symbolicregression.jl,” (2023), arXiv:2305.01582 [astro-ph.IM].
- [36] S.-M. Udrescu and M. Tegmark, *Sci. Adv.* **6**, eaay2631 (2020), arXiv:1905.11481 [physics.comp-ph].
- [37] A. Sousa-Neto, C. Bengaly, J. E. Gonzalez, and J. Alcaniz, *Phys. Dark Univ.* **50**, 102108 (2025), arXiv:2502.10506 [astro-ph.CO].
- [38] S. M. Koksang and A. Heinesen, (2026), arXiv:2604.05822 [astro-ph.CO].
- [39] D. J. Bartlett, H. Desmond, and P. G. Ferreira, *IEEE Trans. Evol. Comput.* **28**, 964 (2024), arXiv:2211.11461 [astro-ph.CO].
- [40] D. Blas, J. Lesgourgues, and T. Tram, *JCAP* **07**, 034 (2011), arXiv:1104.2933 [astro-ph.CO].
- [41] See Supplemental Material at [URL will be inserted by publisher] for details of the symbolic-regression setup, the resolution estimate, and the full Pareto-front results.
- [42] C. Stahl, D. Werth, and V. Poulin, *Phys. Rev. D* **111**, 123514 (2025), arXiv:2502.02571 [astro-ph.CO].
- [43] R. Calderon, T. Simon, A. Shafieloo, and D. K. Hazra, *JCAP* **01**, 057 (2026), arXiv:2504.06183 [astro-ph.CO].
- [44] Note that the MCMC results depend on the choice of priors, in particular on  $\omega_X$ , which is not equivalent across the three templates; the comparison should therefore be regarded as heuristic.
- [45] J. Torrado and A. Lewis, *JCAP* **05**, 057 (2021), arXiv:2005.05290 [astro-ph.IM].
- [46] Y.-S. Piao and Y.-Z. Zhang, *Phys. Rev. D* **70**, 063513 (2004), arXiv:astro-ph/0401231.
- [47] M. Baldi, F. Finelli, and S. Matarrese, *Phys. Rev. D* **72**, 083504 (2005), arXiv:astro-ph/0505552.
- [48] Y. Cai and Y.-S. Piao, *Phys. Rev. D* **103**, 083521 (2021),

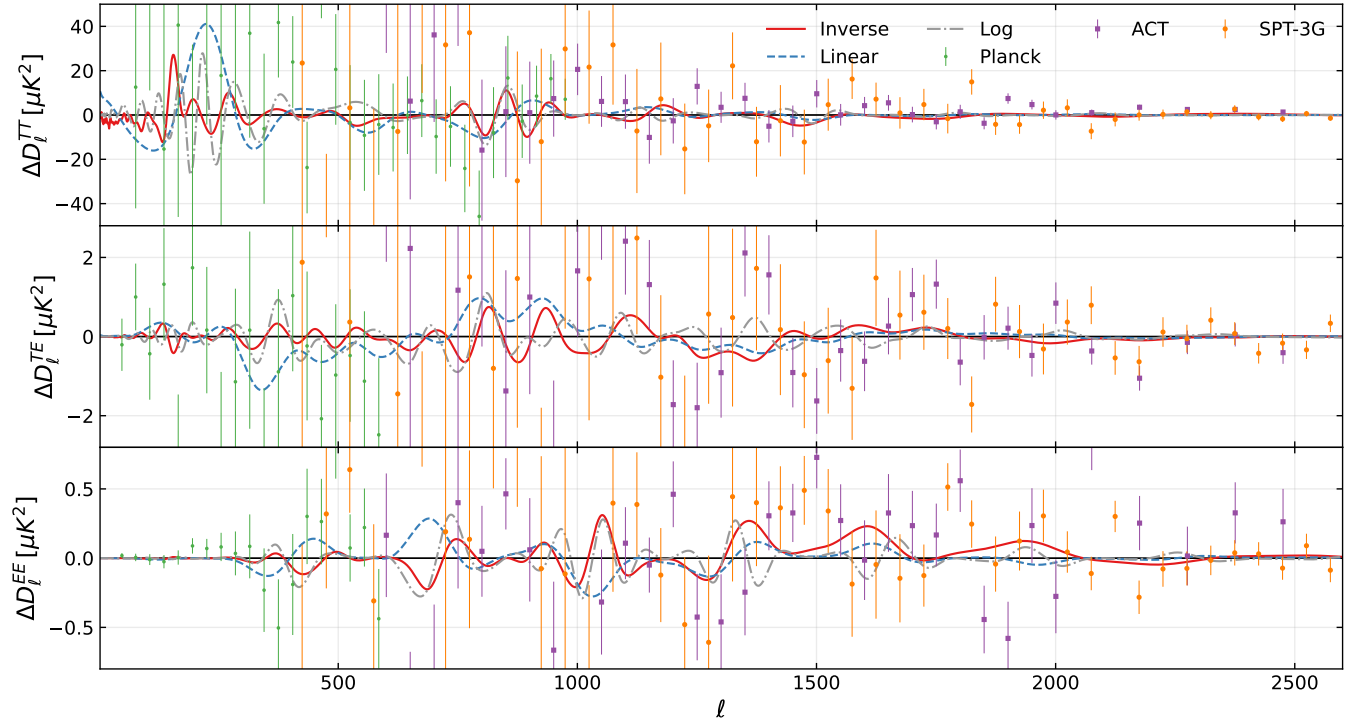


FIG. 4. CMB residuals of the best-fit linear, logarithmic and inverse- $k$  templates relative to the no-feature SPA baseline, compared with the Planck (cropped), ACT and SPT-3G data.

- arXiv:2012.11304 [gr-qc].
- [49] G. Ye, M. Zhu, and Y. Cai, *JHEP* **02**, 008 (2024), arXiv:2312.10685 [gr-qc].
- [50] Y. Cai, M. Zhu, and Y.-S. Piao, *Phys. Rev. Lett.* **133**, 021001 (2024), arXiv:2305.10933 [gr-qc].
- [51] S. Pan, Y. Cai, and Y.-S. Piao, *Eur. Phys. J. C* **84**, 976 (2024), arXiv:2404.12655 [astro-ph.CO].
- [52] P. Ade *et al.* (Simons Observatory), *JCAP* **02**, 056 (2019), arXiv:1808.07445 [astro-ph.CO].
- [53] K. Abazajian *et al.*, (2019), arXiv:1907.04473 [astro-ph.IM].

## Supplemental Material for “Inverse- $k$ Primordial Oscillations from a Symbolic Regression Search”

### Details of the SR search

We write the primordial power spectrum (PPS) as

$$P_{\mathcal{R}}(k) = P_{\mathcal{R},0}(k) [1 + f(k)] \quad (6)$$

and  $f(k)$  is the primordial feature we search for. We use  $k$  in  $\text{Mpc}^{-1}$  as the input variable of PySR. For a given expression  $f(k)$ , the primordial spectrum is supplied to CLASS as an external spectrum and the objective function is the CMB  $\chi^2$  with the background and nuisance parameters fixed to their best-fit values.

The operator set used in the SR search is

$$+, \quad -, \quad \times, \quad /, \quad \wedge, \quad (, \quad ) \quad (7)$$

and

$$\exp, \quad \log, \quad \sin, \quad \cos, \quad \tanh. \quad (8)$$

Nested trigonometric functions are forbidden, and the maximum expression size is set to 25.

The finite sampling limits the frequency that can be reliably resolved. For the sake of efficiency, we set `k_per_decade_primordial=400` in CLASS. For an inverse- $k$  phase,  $\phi(k) = B/k$ , the phase variation over one CLASS sampling step is approximately

$$|\Delta\phi| \simeq \frac{B}{k} \Delta \ln k, \quad \Delta \ln k = \frac{\ln 10}{400}. \quad (9)$$

For  $B \simeq 4 \text{Mpc}^{-1}$ , this gives  $|\Delta\phi| \lesssim 1$  for  $k \gtrsim 0.02 \text{Mpc}^{-1}$ . The inverse- $k$  C8 solutions are therefore numerically stable over the main CMB-sensitive range. Higher-complexity Planck expressions containing inverse powers such as  $1/k^2$  oscillate faster at small  $k$  and are not considered as robust physical results.

### Full SR results

Complexity	$\chi_{\text{Planck}}^2$	$f(k)$
1	606.52	$2.90 \times 10^{-4}$
5	606.40	$-0.00957k^2$
6	605.51	$0.00197/\cos k$
7	604.13	$\sin(1.110k^2)$
8	596.84	$-0.0299 \cos(4.101/k)$
10	595.08	$-0.0339 \cos(4.150/k - 0.859)$
11	593.42	$k \sin(-0.868/k^2)$
13	591.82	$k \sin[-0.868/(k^2 + 8.89 \times 10^{-6}k)]$
16	585.17	$0.0924 \sin[(2.990 + 0.5248/k)/k]$
18	585.17	$0.0924 \sin(2.990/k + 0.5248/k^2)$
19	585.15	$0.0924 \sin[(0.5248 + 2.990k)/k^2]$

TABLE V. Full Pareto-front expressions from the Planck SR run.

The full Pareto-front expressions from the Planck and SPA SR runs are listed in Tables V and VI, respectively.

Complexity	$\chi_{\text{SPA}}^2$	$f(k)$
1	463.90	$2.22 \times 10^{-4}$
3	463.84	$0.00527k$
5	463.79	$0.0133k - 7.31 \times 10^{-4}$
7	457.85	$-0.0106 \sin(-390.0k)$
8	451.70	$-0.0209 \sin(4.231/k)$
10	451.33	$0.0209 \sin(4.178/k - 2.594)$
15	450.67	$0.0218 \sin(4.173/k + 4.173/e^k)$
24	450.34	$0.0219 \sin(4.165/k + 4.266/e^k)$

TABLE VI. Full Pareto-front expressions from the SPA SR run.